

This article was downloaded by:

On: 28 January 2011

Access details: *Access Details: Free Access*

Publisher *Taylor & Francis*

Informa Ltd Registered in England and Wales Registered Number: 1072954 Registered office: Mortimer House, 37-41 Mortimer Street, London W1T 3JH, UK



Physics and Chemistry of Liquids

Publication details, including instructions for authors and subscription information:

<http://www.informaworld.com/smpp/title~content=t713646857>

Electrochemical redox pattern and allied interactive behaviour of FAD on a ruthenium-modified glassy carbon electrode surface

Haizhen Wei^a; Hongbing Tan^b; Yanwei Zeng^a

^a College of Materials Science and Engineering, Nanjing University of Technology, Nanjing 210009, P.R. China ^b State Key Laboratory of Hydrology-Water Resources and Hydraulic Engineering, Hohai University, Nanjing 210098, P.R. China

Online publication date: 10 December 2010

To cite this Article Wei, Haizhen , Tan, Hongbing and Zeng, Yanwei(2010) 'Electrochemical redox pattern and allied interactive behaviour of FAD on a ruthenium-modified glassy carbon electrode surface', *Physics and Chemistry of Liquids*, 48: 6, 708 – 722

To link to this Article: DOI: 10.1080/00319100902929227

URL: <http://dx.doi.org/10.1080/00319100902929227>

PLEASE SCROLL DOWN FOR ARTICLE

Full terms and conditions of use: <http://www.informaworld.com/terms-and-conditions-of-access.pdf>

This article may be used for research, teaching and private study purposes. Any substantial or systematic reproduction, re-distribution, re-selling, loan or sub-licensing, systematic supply or distribution in any form to anyone is expressly forbidden.

The publisher does not give any warranty express or implied or make any representation that the contents will be complete or accurate or up to date. The accuracy of any instructions, formulae and drug doses should be independently verified with primary sources. The publisher shall not be liable for any loss, actions, claims, proceedings, demand or costs or damages whatsoever or howsoever caused arising directly or indirectly in connection with or arising out of the use of this material.

Electrochemical redox pattern and allied interactive behaviour of FAD on a ruthenium-modified glassy carbon electrode surface

Haizhen Wei^{a*}, Hongbing Tan^b and Yanwei Zeng^a

^aCollege of Materials Science and Engineering, Nanjing University of Technology, Nanjing 210009, P.R. China; ^bState Key Laboratory of Hydrology-Water Resources and Hydraulic Engineering, Hohai University, Nanjing 210098, P.R. China

(Received 12 January 2009; final version received 27 March 2009)

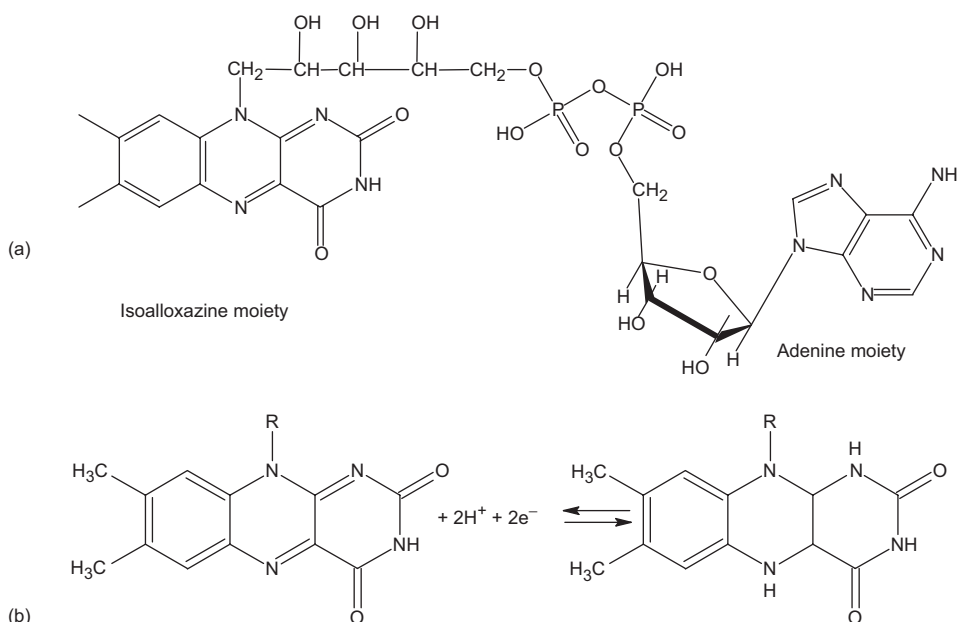
The redox and interactive behaviour of flavin adenine dinucleotide (FAD) with a ruthenium (Ru)-modified glassy carbon electrode (GCE) was investigated. The electron-transfer kinetics on the Ru-modified GCE gives an apparent electron-transfer coefficient, α_{app} of 0.56, and an apparent heterogeneous electron transfer rate constant, k_{app} of 2.32 s^{-1} , respectively. The cyclic voltammetry (CV) complemented by alternating cyclic voltammetry (ACV) shows reduction of FAD to be a quasi-reversible reaction involving FAD adsorption. The adsorption of FAD on the Ru-modified GCE fits a Langmuir adsorption isotherm. The large apparent negative Gibbs energy of adsorption ΔG_{ads} ($-38.2 \text{ kJ mol}^{-1}$) of FAD onto the Ru-modified GCE confirmed a strong chemical adsorption of FAD on the surface. The deposited Ru islands block surface sites for FAD adsorption and the electron-transfer communication between FAD and the electrode surface does not significantly improve with a deposited Ru monolayer.

Keywords: flavin adenine dinucleotied (FAD); Ru-modified glassy carbon electrode; adsorptive thermodynamics; electron-transfer kinetics

1. Introduction

Flavin adenine dinucleotide (FAD) is a derivative of vitamin B₂ (VB₂) with the 7,8-diethylisoalloxazine structure (Scheme 1(a)) and is an important coenzyme for many oxidoreductases [1]. To develop an enzyme-electrode for electrochemical biosensors and enzymatically based technological processes, the direct interaction of FAD with various conducting and semi-conducting materials, such as carbon nanotubes, mercury, platinum, graphite, etc., has been investigated [1–9]. Several approaches on electrode modification, such as covalent coupling and irreversible adsorption, have improved the effectiveness of electron-transfer communication between FAD and electrode [10–14]. However, such modified electrodes lack long-term stability and durability because the modification layer is lost when oxidation/reduction reaction occurs [15]. Therefore, it is of interest to design a metal-modified electrode with long-term stability and high efficiency in electron-transfer for

*Corresponding author. Email: whz0803@yahoo.com.cn



Scheme 1. (a) Flavin adenine dinucleotide (FAD). (b) FAD redox process involving the isoalloxazine moiety.

enzymatically based technological processes. In this work, a glassy carbon electrode (GCE) was chosen being one of the most commonly used electrodes in electrochemical biosensors. Ruthenium (Ru) was chosen because it forms an H–Ru bond of an intermediate strength, ensuring high coverage with hydrogen at low over potentials allowing it to desorb using little energy [15,16].

Previously, studies on the interaction of FAD with a GCE considered FAD adsorption thermodynamics and kinetics and the electroreduction mechanism [17]. The interactive behaviour and the electron-transfer kinetics of FAD at a Ru-modified GCE are discussed here. The difference in FAD interactive behaviour between the FAD/GCE and FAD/Ru-modified GCE is compared using various electrochemical techniques, and considers the possibility of designing a flavoenzyme electrode for enzymatically based technological processes.

2. Experimental part

2.1. Chemicals and reagents

Electrochemical studies used a 0.05 M phosphate buffer, pH = 7.0 (if otherwise not stated). The buffer was prepared by dissolving monobasic KH_2PO_4 (Sigma, P-5379) in ultra-pure de-ionised water (resistivity 18.2 $\text{M}\Omega\text{cm}$) and adding 0.10 M sodium hydroxide (APC Chemical Inc.) to adjust pH. Stock solutions of FAD (disodium salt, purity 98%, Sigma 146-14-5) were prepared in a separate container by dissolving a correct amount of the reagent in the supporting electrolyte (phosphate buffer). The chemicals were not further purified.

2.2. Electrochemical cell, electrodes and instruments

A standard three-electrode, two-compartment 50 mL electrochemical cell was used. The counter electrode was a large-area platinum electrode of high purity (99.99%, Johnson–Matthey), which was degreased by refluxing in acetone, sealed in soft glass, electrochemically cleaned by potential cycling in 0.5 M sulphuric acid, and stored in 98% sulphuric acid. During the measurement, the counter electrode was separated from the main cell compartment by a glass frit. The reference electrode was a saturated calomel electrode (SCE), to which all potentials are referred. The working electrode was a GCE (BAS Instruments Ltd, Geometric area, $A=0.2826\text{ cm}^2$). Before each experiment, the GCE was polished with diamond paste down to $0.03\text{ }\mu\text{m}$ gradation, followed by rinsing with de-ionised water, ethanol and cleaning in an ultrasonic bath for 5 min in order to remove polishing residues. The electrode was then electrochemically pretreated (activated) in 0.5 M sulphuric acid by potentiodynamic cyclic polarisation (100 cycles) between -1.4 and 1.9 V at a scan rate of 100 mV s^{-1} . While not in use, all the glassware was stored in 98% sulphuric acid.

Electrochemical techniques of cyclic voltammetry (CV), differential pulse voltammetry (DPV), alternating cyclic voltammetry (ACV) and Chronopotentiometry (CE) were employed using an Autolab potentiostat/galvanostat/frequency_response_analyser (Ecochemie), PGSTAT30, controlled by the GPES/FRA v.4.9.5 software. A sub-monolayer of Ru was potentiostatically deposited onto the prepared GCE at -0.2 V versus SCE from a 1 mM RuCl_3 solution in $0.5\text{ M H}_2\text{SO}_4$.

All the measurements were in an oxygen-free solution, achieved by continuously purging the electrochemical cell with argon gas (99.998% pure) prior the experiment. Measurements were made in a quiescent solution: the inert atmosphere was maintained by saturating the cell above the electrolyte with argon at a room temperature of $22 \pm 1^\circ\text{C}$. Before measurements in a FAD-containing electrolyte, the background response of the electrode was first recorded in phosphate buffer.

3. Results and discussion

3.1. Deposition of Ru on the GCE

Prior to Ru electrodeposition, the surface of the two-dimensional GCE was polished with a diamond paste down to $0.03\text{ }\mu\text{m}$, followed by degreasing with ethanol in an ultra-sound bath and electrochemical activation in $0.5\text{ M H}_2\text{SO}_4$ by potentiodynamic polarisation between -1.4 and 1.9 V for 40 cycles with scan rate of 100 mV s^{-1} . A sub-monolayer of Ru was potentiostatically deposited onto the prepared GCE from a 1 mM RuCl_3 solution in $0.5\text{ M H}_2\text{SO}_4$ at -0.2 V for different time period as shown in the inset in Figure 1.

Figure 1 shows cyclic voltammograms of the electrode recorded in 0.5 M phosphate buffer. Two anodic peaks correspond to desorption of hydrogen adsorbed on Ru sites of the electrode (A1), and oxidation of metallic Ru to RuOH (A2), in agreement with literature [15,18,19]. In the reverse scan, two weak cathodic peaks were recorded, corresponding to the reduction of Ru-oxides formed (C2), and adsorption of hydrogen on Ru sites of the electrode (C1). The Ru coverage was roughly estimated by measuring the oxidation charge of the Ru sub-monolayer [after subtraction for the double-layer charge in the potential range of

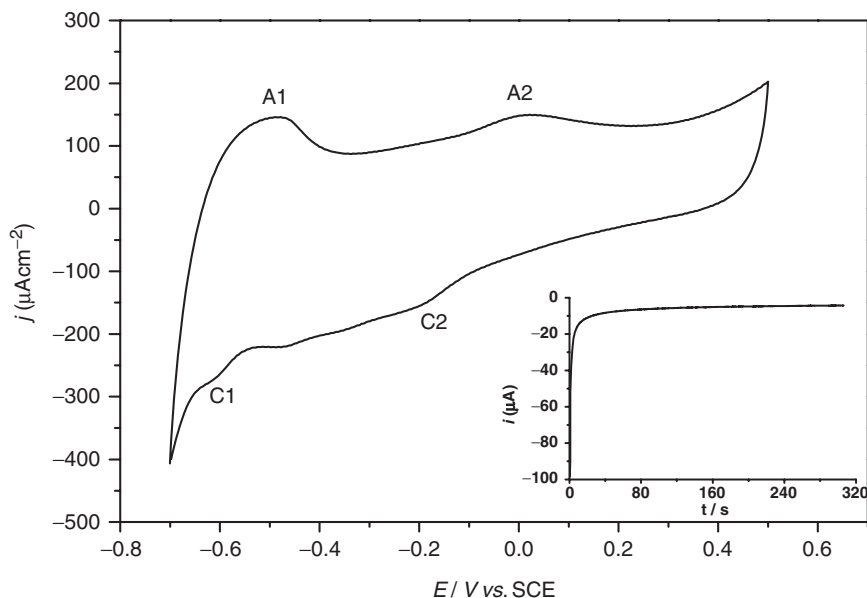


Figure 1. Cyclic voltammograms of Ru-modified GCE in 0.5M phosphate buffer solution pH 7.0. Scan rates, $\nu = 100 \text{ mV s}^{-1}$. Temperature, $T = 295 \text{ K}$. Inset: Chrono potentiometry for electrochemical deposition of Ru on GCE. Pretreatment procedure: first conditioning potential = 0.66 V, duration time = 5 s. Measurement: interval time = 1 s, potential = -0.2 V.

-0.23 to 0.20 V ($86.3 \mu\text{C cm}^{-2}$)]. Assuming the reaction of Ru to RuOH ($\text{Ru} + \text{H}_2\text{O} \rightarrow \text{RuOH} + \text{H}^+ + \text{e}^-$) to give peak A2 [20,21], and with the charge to form a monolayer of RuOH as $249 \mu\text{C cm}^{-2}$ [18,19], the value of the degree of deposition was estimated.

For comparison, cyclic voltammograms of the bare GCE (a) and Ru-modified GCE (b) recorded in phosphate buffer in the potential range of -0.7 to -0.2 V are shown in Figure 2. The well-defined cyclic voltammogram peak recorded at ca -0.5 V in a FAD containing solution using the Ru-modified GCE (curve (c), Figure 2) gives the FAD/FADH₂ redox reaction for the exchange of two electrons and two hydrogens per FAD molecule (Scheme 1(b)). The electron-transfer mechanism will be discussed later.

3.2. Redox and interactive behaviour of FAD at a Ru-modified GCE surface

3.2.1. Cyclic voltammetry

A set of cyclic voltammograms of a Ru-modified GCE in phosphate buffer pH = 7.0 containing 50 μM of FAD at scan rates were recorded (Figure 3). Obviously, the separation between the cathodic and anodic peaks, ΔE_p , increases with an increase in scan rate (ν), and the plot of ΔE_p versus ν shows a linear relationship ($\Delta E_p = 0.105\nu + 0.038$, $R^2 = 0.9922$), revealing the reduction of FAD on a Ru-modified GCE to be a quasi-reversible reaction.

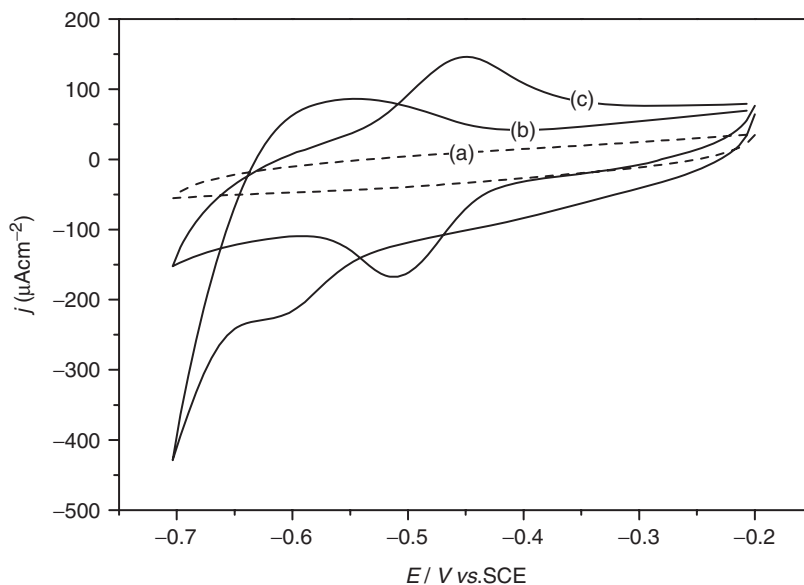


Figure 2. Cyclic voltammograms of (a) bare GCE in 0.5 M phosphate buffer solution pH 7.0; (b) Ru-modified GCE in 0.5 M phosphate buffer solution pH 7.0; (c) Ru-modified GCE in phosphate buffer containing 100 μM FAD. Scan rates, $\nu = 100 \text{ mV s}^{-1}$. Temperature, $T = 295 \text{ K}$.

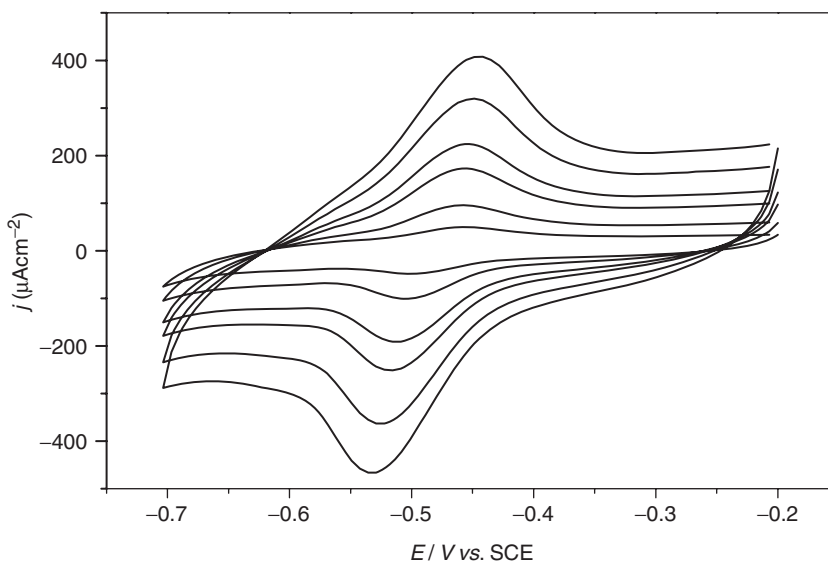


Figure 3. Cyclic voltammograms of a Ru-modified GCE in phosphate buffer pH = 7.0 containing 50 μM of FAD recorded at scan rates of $\nu = 40, 80, 150, 200, 300, 400 \text{ mV s}^{-1}$ (from inner to outer).

The quasi-reversibility could be related to the rate of electron-transfer process between the electrode surface and the FAD/FADH₂ molecules, or to sluggish mass transport of FAD molecules either in the bulk electrolyte or on the electrode surface. Whether the FAD reduction is surface-controlled or mass-transport-controlled process depends on how the cathodic and anodic peak current of the CVs react to the corresponding scan rate in various concentration of FAD (e.g. 10, 50 and 100 μM) (Figure 4). The graph shows both the cathodic and anodic peak current vary linearly with scan rate (ν). Therefore, both the FAD reduction and FADH₂ oxidation are surface-controlled (adsorptive) process instead of mass-transport process in the dilute solution. The results from alternating cyclic voltammetry (ACV) complement this conclusion as is discussed later (Section 3.2.2).

Figure 4 shows that adsorption of FAD on the Ru-modified GCE is one reaction step in the reaction mechanism. Consequently, the dependence of the peak current on the concentration of FAD bulk solution should display an isotherm-like shape. Therefore, to investigate the isotherm of FAD adsorption on the Ru-modified GCE, CV measurement were made for a wide FAD concentration range at a constant scan rate (ν), and the corresponding results are presented in Figure 5. The set of CVs shows that an increase in FAD concentration in the bulk solution increases the peak current in both anodic (not shown) and cathodic scan: the graph shows a classic adsorptive behaviour. The surface concentration of adsorbed FAD, Γ (mol cm^{-2}), was calculated by integrating the area (i.e. charge) under the cathodic peak and using the well-known Faraday equation: $Q = nFA\Gamma$ [22].

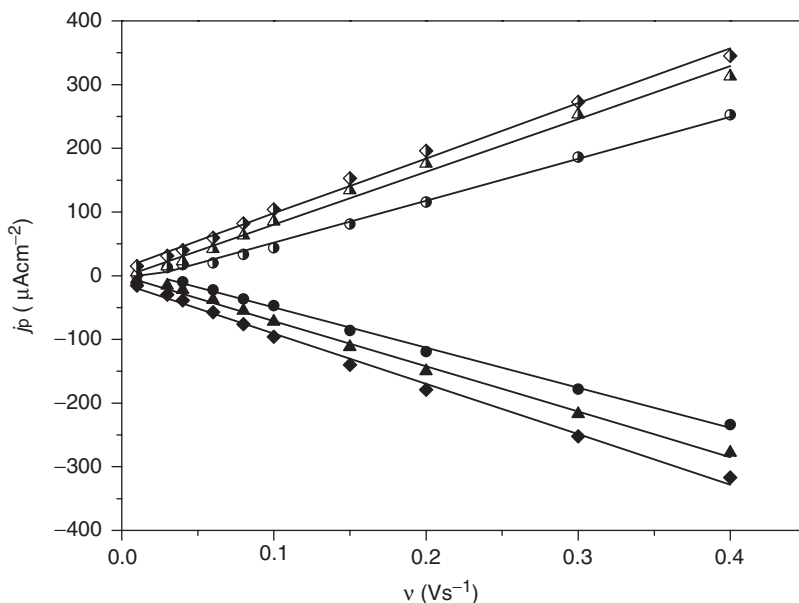


Figure 4. Dependence of the anodic (semi-solid symbols) and cathodic (solid symbols) peak current on the applied scan rate in various FAD concentrations: 10, 50, 100 μM . Data obtained from the cyclic voltammograms presented in Figure 3 and others non-presented voltammograms and the solid line is the linear fit.

The adsorption isotherm is obtained from the condition of equality of electrochemical potentials for bulk and adsorbed FAD species at equilibrium [22]:

$$\mu_i^{-A} = \mu_i^{-b},$$

where the superscripts A and b refer to adsorbed i and bulk i , respectively.

In this case, using the calculated surface concentration values, the dependence of the surface concentration of adsorbed FAD molecules on equilibrium FAD-bulk concentration shows an isotherm-type behaviour (Figure 5(a)), and the adsorption process was modelled by a suitable adsorption isotherm. Several isotherm, such as the logarithmic Temkin isotherm, the Langmuir isotherm and the Frumkin isotherm have been tested, and the Langmuir isotherm [23] [Equation (1)] gave the best agreement between the experimental and model values as shown in the inset (a) in Figure 5. It means the adsorption process satisfied all assumptions of the Langmuir isotherm: (a) no interactions between the adsorbed species on the electrode surface; (b) no heterogeneity of the surface; and (c) at high bulk activities, saturation coverage of the electrode by adsorbate (e.g. to form a monolayer) of amount Γ_{\max} .

$$\Gamma_i = \frac{\Gamma_{\max} B_{\text{ads}} c}{1 + B_{\text{ads}} c}. \quad (1)$$

By rewriting Equation (1) to yield the linearised form (Equation (2)) as below:

$$\frac{c}{\Gamma_i} = \frac{1}{\Gamma_{\max} B_{\text{ads}}} + \frac{c}{\Gamma_{\max}}, \quad (2)$$

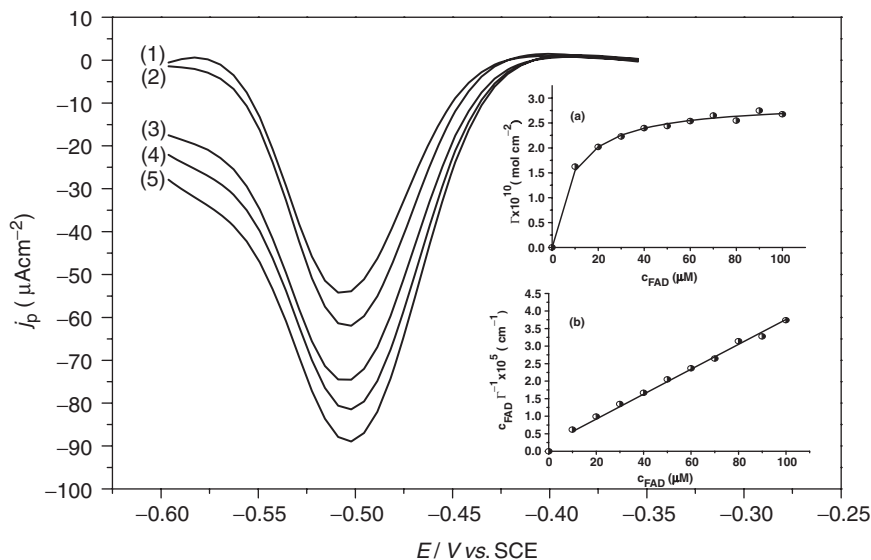


Figure 5. Cyclic voltammograms of Ru-modified GCE in phosphate buffer pH 7.0 containing various concentrations of FAD: (1) 20, (2) 40, (3) 60, (4) 80, (5) 100 μM . Scan rate, $\nu = 100 \text{ mV s}^{-1}$; first condition potential = 0 V; equilibrium time = 5 s. Temperature, $T = 295 \text{ K}$. Inset: (a) Dependence of the surface concentration of FAD on the corresponding equilibrium concentration of FAD. Inset (b) Linearised Langmuir adsorption isotherm. The symbols represent the experimental data and the line is the modelled Langmuir isotherm.

where Γ_i (mol dm^{-2}) is the FAD surface concentration at the corresponding equilibrium concentration of FAD in the bulk solution c ($\text{mol L}^{-1} = \text{M}$), Γ_{max} is the surface concentration at the maximum (saturated) FAD surface coverage and the parameter B_{ads} (M^{-1}), the adsorption affinity constant, reflects the affinity of FAD towards GCE surface adsorption sites at a constant temperature.

Consequently, if the adsorption of FAD on the Ru-modified GCE surface fits the Langmuir isotherm, a plot of c/Γ_i versus c should yield a straight line: the plotted c/Γ_i versus c is linear (mean correlation coefficient, $R^2 = 0.997$) [Inset (b)], and the dependence shows an isotherm-type behaviour and a Langmuir isotherm (line) well describes the adsorption process of FAD on the surface. The adsorption affinity constant, B_{ads} , is derived from the slope and the intercept to be $1.11 \times 10^5 \text{ M}^{-1}$ and correspondingly, the Gibbs free energy is calculated to be 38.3 kJ mol^{-1} based on the following equation:

$$B_{\text{ads}} = \frac{1}{55.5} \exp\left(\frac{-\Delta G_{\text{ads}}}{RT}\right), \quad (3)$$

where R ($\text{J mol}^{-1} \text{ K}^{-1}$) is the gas constant, T (K) is the temperature, ΔG_{ads} (J mol^{-1}) is the Gibbs energy of adsorption and 55.5 is the molar concentration of a solvent (water in this case, mol dm^{-3}).

3.2.2. Alternating cyclic voltammetry

Alternating cyclic voltammetry (ACV) investigated the interaction of FAD on Ru-modified GCE for various concentrations and many potentials. The resulting differential capacitance against applied potential curves was obtained using the following equation [15] (Figure 6):

$$C = I/(2\pi fA), \quad (4)$$

where C (F cm^{-2}) is the capacitance; I (A) is the current; f (Hz) is the frequency; A (cm^{-2}) is the electrode area.

The C - E curves obtained at various concentrations of FAD indicate a decrease with increasing of FAD bulk concentration in the double-layer capacitance with respect to the capacitance of the supporting electrolyte. The capacitance curves in the electrochemical double-layer region (ca from -0.2 to -0.35 V) clearly show that a small amount of FAD (e.g. $10 \mu\text{M}$) in the supporting electrolyte gives a significant decrease in capacitance. The measured capacitance further decreases with an increase in FAD bulk solution concentration, direct evidence of the adsorption of FAD on the Ru-GCE electrode surface.

The apparent FAD surface coverage at a constant potential (θ_i) was calculated from capacitance curves. Knowing that $\theta_i = \Gamma_i/\Gamma_{\text{max}}$, the Langmuir isotherm [Equation (2)] can be further rearranged into the linearised form Equation (5):

$$\frac{c}{\theta_i} = \frac{1}{B_{\text{ads}}} + c. \quad (5)$$

The FAD adsorption data from Figure 6 taken in the double-layer region, -0.20 , -0.25 , -0.30 , -0.35 V, are presented in Figure 7. The plotted curves of c/θ versus c at different potentials are linear, giving an overall mean slope of 1.0015 and a mean

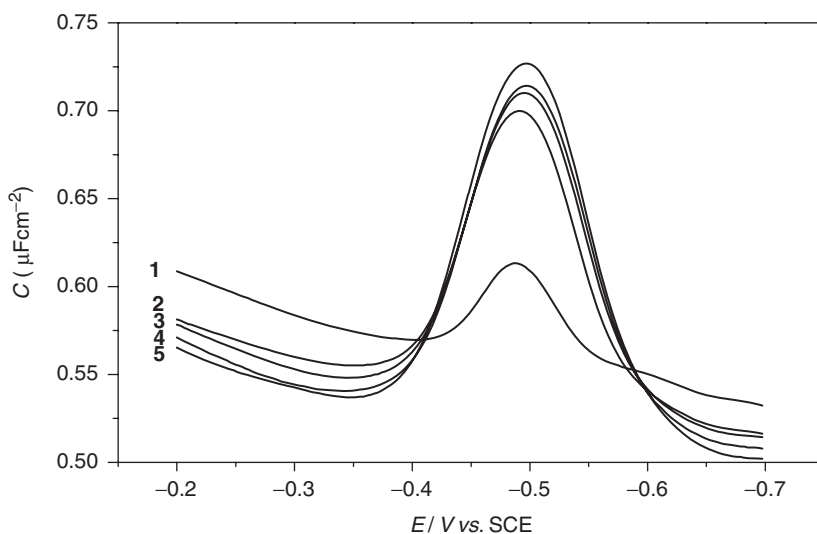


Figure 6. Alternating cyclic voltammograms of Ru-modified GCE recorded in phosphate buffer pH = 7.0 containing various concentration of FAD: (1): 0 μM , (2): 10 μM , (3): 30 μM , (4): 50 μM , (5): 100 μM . Modulation time = 0.16 s; modulation amplitude = 0.005 V_{rms} ; step potential = 0.003 V; phase = 0° ; scan rate, $\nu = 0.005 \text{ V s}^{-1}$; frequency = 25 Hz.

correlation coefficient of $R^2 = 0.9785$. Such excellent agreement shows the Langmuir isotherm describes the adsorption of FAD on to the Ru-modified GCE surface very well. From the slope, an average adsorption affinity constant of $1.08 \times 10^5 \text{ M}^{-1}$ is calculated. Correspondingly, the apparent Gibbs energy of adsorption of FAD onto the Ru-modified GCE is $\Delta G_{\text{ads}} = -38.2 \text{ kJ mol}^{-1}$, in excellent agreement with the values obtained from CV measurements, where $B_{\text{ads}} = 1.11 \times 10^5 \text{ M}^{-1}$ and $\Delta G_{\text{ads}} = -38.3 \text{ kJ mol}^{-1}$.

3.3. Electron-transfer kinetics of FAD at a Ru-modified GCE surface

The oxidative/reductive reaction of FAD at a Ru-modified GCE is under quasi-reversible reaction. A series differential pulse voltammograms obtained in various concentrations was fitted by a kinetic model for quasi-reversible electrochemical reaction using General Purpose Electrochemical software [24], and the detailed information for fit and simulation procedure accounting for a heterogeneous kinetics has been explained by A.J. Bard [22]. During the simulation, parameters in terms of the reaction mechanism and number of exchanged electrons were set firstly according to the reaction mechanism, and the apparent electron-transfer coefficient would be given by an iterative algorithm until the experimental i - E curve is fully fitted by the simulated one.

An excellent agreement between the simulated and experimental voltammograms was obtained for DPV data at different concentrations, 10, 30 and 50 μM . The mean value of the apparent electron-transfer coefficient is calculated to be 0.56 ± 0.04 .

The electrochemical response (the voltammetric i - E curve) for the electrode reaction is affected significantly by the adsorption of oxidant (O) or reductant (R).

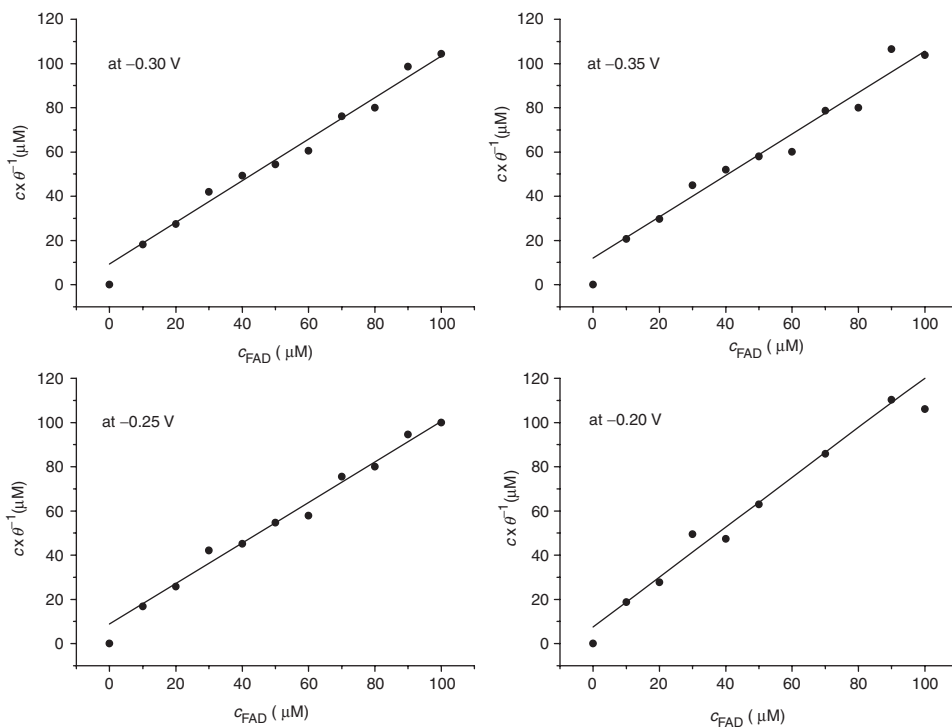


Figure 7. Linearised Langmuir adsorption isotherm obtained from AC voltammograms of Ru-modified GCE recorded at different potential in phosphate buffer pH = 7.0 containing various concentration of FAD.

The theoretical treatments applying cyclic voltammetric methods to the study of surface processes are being discussed in the literature [22,25]. The treatments for the general case of a quasi-reversible reaction involving the adsorption isotherm for both O and R have been discussed and the peak values are given by the followings equation [22]:

$$E_p - E' = \frac{RT}{\alpha_{app} n F} \ln \left(\frac{RT k_{app}}{\alpha n F v} \right), \tag{6}$$

where E' (V) is the formal potential, α_{app} is the electron-transfer coefficient and k_{app} (s^{-1}) is the apparent heterogeneous electron-transfer rate constant for the surface electron transfer.

Using CV data at various scan rates in different FAD concentrations at pH 7.0, yielded a formal FAD reduction potential value of $E' = -0.484$ V. The apparent electron transfer coefficient and heterogeneous electron transfer rate constant can be calculated from the scan-dependent CVs using Equation (6). Figure 8 shows the difference between cathodic peak potential and formal FAD reduction potential ($E_p - E'$) in 100 µM FAD to be proportional to the logarithm of scan rate ($\ln v$). From the slope of the line an apparent electron-transfer coefficient value of $\alpha_{app} = 0.56$ was calculated, which is the same as obtained by the fitting procedure.

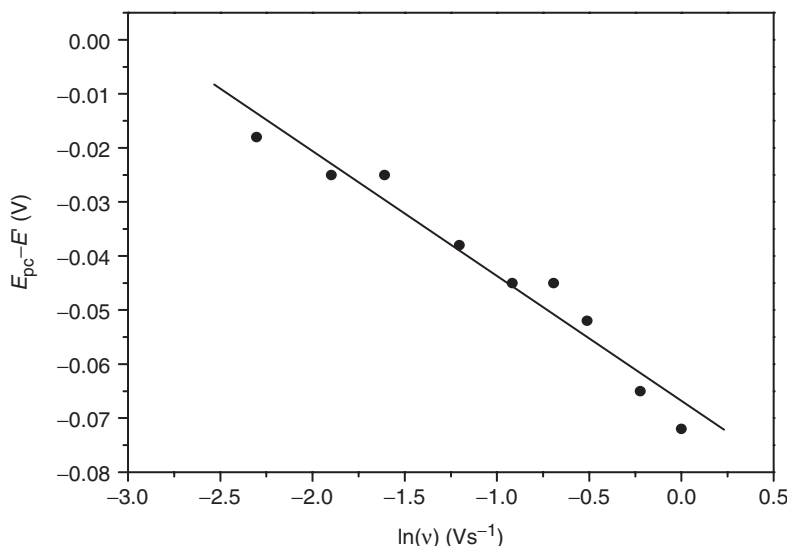


Figure 8. Dependence of the difference between cathodic peak potential and formal FAD reduction potential ($E_p - E'$) on the logarithm of scan rate ($\ln \nu$). The symbols represent the experimental data and the line is the linear fitting data.

The intercept gave an apparent heterogeneous electron transfer rate constant of $k_{app} = 2.32 \text{ s}^{-1}$.

3.4. Comparison of the electrochemical behaviour of FAD with a bare GCE and a Ru-modified GCE

Comparable studies of the electrochemical behaviour of FAD with a bare GCE and the Ru-modified GCE were performed. Figure 9 shows the CV recorded in phosphate buffer pH 7.0 containing $100 \mu\text{M}$ FAD at the bare GCE (curve (a)) to be basically similar to that at the Ru-modified GCE (curve (b)). However, the cathodic (or anodic) peak current of Ru-modified GCE in $100 \mu\text{M}$ FAD is less than that of GCE under the same experimental condition.

The kinetics of FAD electro-reduction at both the bare GCE and the Ru-modified GCE were found to be adsorption-controlled process, thus the faradic current in CV reflects the surface concentration of attached FAD based on the Nernst equation [22]:

$$i = \frac{n^2 F^2 \Gamma A \nu}{4RT}, \quad (7)$$

where n is the number of electrons involved in the redox reaction, F is the Faraday constant, A (cm^2) is the surface area of the electrode, Γ (mol cm^{-2}) is the FAD surface concentration, i (A) is the peak current, ν (Vs^{-1}) is the scan rate, R ($\text{J mol}^{-1} \text{K}^{-1}$) is the gas constant and T (K) is the absolute temperature.

Therefore, the equilibrium surface concentration of FAD at the Ru-modified GCE in a specific concentration of bulk solution is less than that at the bare GCE

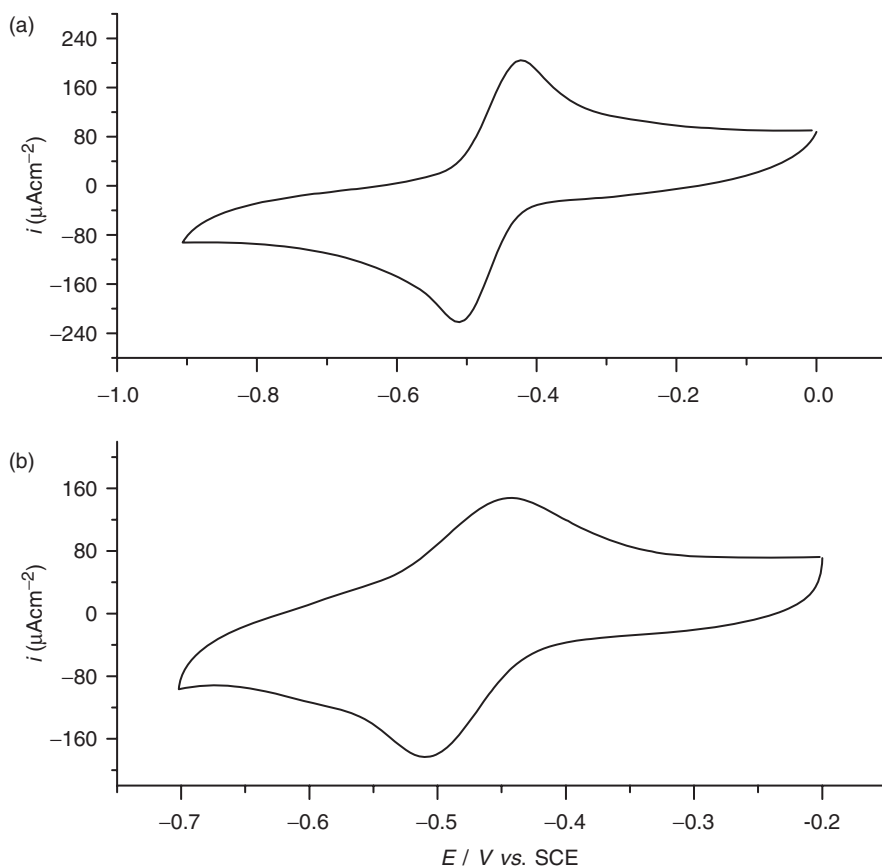


Figure 9. Cyclic voltammograms of (a) the bare GCE and (b) the Ru-modified GCE in phosphate buffer pH=7.0 containing 100 μM of FAD recorded at scan rates of $\nu = 100 \text{ mV s}^{-1}$.

surface. It is confirmed by the recorded CVs of Ru-modified GCE with different deposition degree of Ru. When the bare GCE was potentiostatically deposited on the electrode surface for different time period, the different deposition degree of Ru-submonolayer was obtained correspondingly. As shown in Figure 10, the cathodic peak current of Ru-modified GCE in 100 μM FAD solution decreases to 90 from 136.31 $\mu\text{A cm}^{-2}$ when the deposition degree of Ru on GCE increases to 22 from 0%. In addition, the equilibrium surface concentration of FAD (Γ , mol cm^{-2}) on the Ru-modified GCE, with different deposition degree of Ru-submonolayer, was calculated from the scan-dependent CVs in same bulk solution using the Nernst equation. The inset in Figure 10 and Table 1 clearly show that the equilibrium surface concentration of FAD decreases linearly with increasing of deposition degree of Ru on the GCE. This further proves that the deposited Ru islands might block partial surface sites for FAD adsorption.

The Gibbs free energy of FAD adsorption on the Ru-modified GCE surface with 22.2% Ru deposition ($-38.3 \text{ kJ mol}^{-1}$) is lower than that of bare GCE surface ($-39.7 \text{ kJ mol}^{-1}$), and the apparent electron-transfer coefficient and apparent

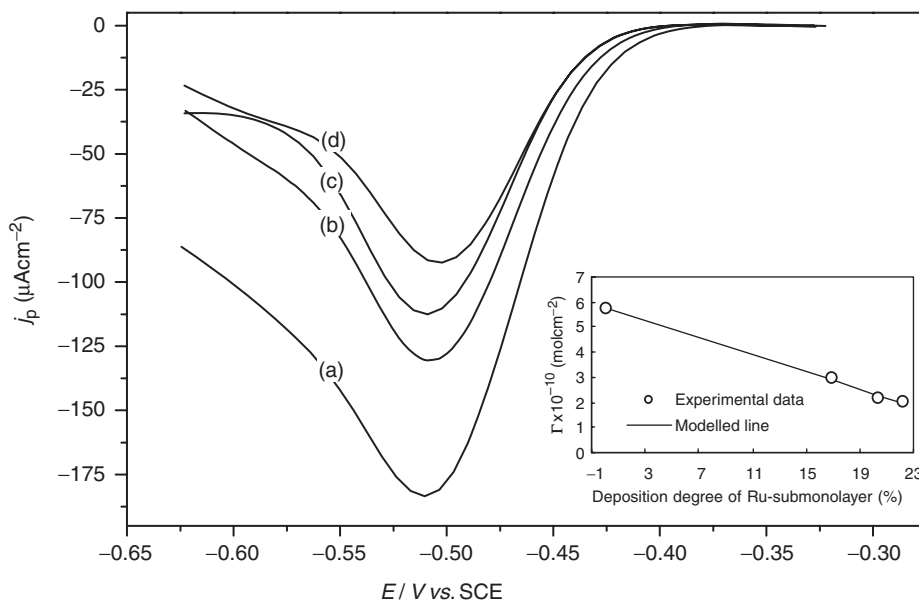


Figure 10. Normalised cyclic voltammograms of Ru-modified GCE with different deposition degree of Ru-submonolayer: (a) 0, (b) 16.9, (c) 20.4, (d) 22.2% recorded in 0.05 M phosphate buffer containing 100 μM FAD. Scan rate, $\nu = 100 \text{ mV s}^{-1}$. Inset: Dependence of the surface concentration of FAD on the deposition degree of Ru-submonolayer obtained from CV with various scan rates.

Table 1. The equilibrium surface coverage of FAD on Ru-modified GCE with different deposition degree of Ru-submonolayer in 100 μM FAD bulk solution.

Deposition time (minute)	Deposition degree of Ru (%)	I_{pc} ($\mu\text{A cm}^{-2}$)	$\Gamma \times 10^{-10}$ (mol cm^{-2})
0	0	136.31	5.74
5	16.9	125.73	3.77
10	20.4	95.75	2.19
25	22.2	90.13	2.02

heterogeneous electron transfer rate constant of $k_{\text{app}} = 2.32 \text{ s}^{-1}$ and $\alpha_{\text{app}} = 0.56$ between the Ru-modified GCE and FAD are higher than that between the bare GCE and FAD where $k_{\text{app}} = 1.4 \text{ s}^{-1}$ and $\alpha_{\text{app}} = 0.41$. It can be concluded that the stronger adsorption of FAD on GCE surface occurs, the slower electron transfer.

The size distribution of Ru islands on a GCE is between *ca* 10 and 40 nm [15]. The adenine ring of FAD directly attached onto GCE surface with a flat orientation and the area of adenine ring is *ca* 50–60 \AA^2 [26]. The possible process for adsorption and the reduction and oxidation of FAD on the Ru-modified GCE is that FAD molecules adsorbs on spots left empty by Ru islands because the adsorption of FAD on a metallic solid electrode surface is weak; the effective adsorption occurs at the interface between FAD and GCE surface, not on the interface between FAD and Ru

sites on the electrode surface. Meanwhile, the electron transfer between FAD molecules and the electrode surface (i.e. reduction step) is enhanced by the presence of deposited Ru because it yields hydrogen using little energy after adsorbing hydrogen at a low cathodic over-potential.

4. Conclusions

The interactive behaviour of FAD with a Ru-modified GCE was studied using CV, DPV and ACV. The reduction of FAD at a Ru-modified GCE surface is a quasi-reversible and surface-controlled process: the FAD adsorption is the rate determining step in the overall reaction mechanism. The adsorption process was described using the Langmuir adsorption isotherm, and the agreement between the Langmuir isotherm and experimental data is excellent for the whole electrochemical double-layer potential region. The apparent negative Gibbs energy of adsorption of FAD onto the Ru-modified GCE of $\Delta G_{\text{ads}} = -38.2 \text{ kJ mol}^{-1}$ is obtained for both CV and ACV technique. This is less than that for FAD on the bare GCE, $\Delta G_{\text{ads}} = -39.7 \text{ kJ mol}^{-1}$. The apparent electron-transfer coefficient and apparent heterogeneous electron transfer rate constant of $k_{\text{app}} = 2.32 \text{ s}^{-1}$ and $\alpha_{\text{app}} = 0.56$ between the Ru-modified GCE and FAD are higher than that between FAD and bare GCE. The results show that the deposited Ru islands does not significantly help the electron-transfer between FAD molecules and the electrode surface. Under the same experimental condition, the surface concentration of FAD on the electrode surface decreases with increase in deposition degree of Ru, therefore the effective adsorption occurs on the interface between FAD and GCE surface rather than between FAD and Ru sites on the electrode surface: the deposited Ru islands block functional surface for the adsorption of FAD on the electrode surface.

Acknowledgements

Grateful acknowledgment is made to the Natural Science and Engineering Research Council of Canada and Quebec Merit Fellowship, and the National Natural Science Foundation of China (No. 40603007) for support of this research. The authors sincerely thank the reviewers for providing valuable comments on the manuscript.

References

- [1] C.S. Lin, R.Q. Zhang, and T.A. Niehaus, Th. Frauenheim, *J. Phys. Chem. C* **111**, 4069 (2007).
- [2] V.I. Birss, S. Guba-Thakurta, C.E. McGarvey, S. Quach, and P. Vanysek, *J. Electroanal. Chem.* **423**, 13 (1997).
- [3] M.M. Kamal, H. Elzanowska, M. Gaur, O. Kim, and V.I. Birss, *J. Electroanal. Chem.* **318**, 349 (1991).
- [4] C. McGarvey, S. Beck, S. Quach, V.I. Birss, and H. Elzanowska, *J. Electroanal. Chem.* **456**, 71 (1998).
- [5] L.T. Kubota, L. Gorton, A. Roddick-Lanzilotta, and A.J. McQuillan, *Bioelectrochem. Bioener.* **47**, 39 (1998).
- [6] Y. Wang, G.Y. Zhu, and E.K. Wang, *Anal. Chim. Acta* **338**, 97 (1997).

- [7] L. Gorton and G. Johnsson, *J. Electroanal. Chem.* **113**, 151 (1980).
- [8] O. Miyawaki and L.B. Wingard, *Biotechnol. Bioeng.* **26**, 1364 (1984).
- [9] O. Miyawaki and L.B. Wingard, *Biochim. Biophys.* **838**, 60 (1985).
- [10] I. Willner, V. Heleg-Shabtai, R. Blonder, E. Katz, G. Tao, A.F. Buckmann, and A. Heller, *J. Am. Chem. Soc.* **118**, 10321 (1996).
- [11] M. Zayats, E. Katz, and I. Willner, *J. Am. Chem. Soc.* **124**, 2120 (2002).
- [12] A.A. Karyakin, Y.N. Ivanova, K.V. Revunova, and E.E. Karyakina, *Anal. Chem.* **76**, 2004 (2004).
- [13] G.Z. Liu, M.N. Paddon-Row, and J.J. Gooding, *Electrochem. Commun.* **9**, 2218 (2007).
- [14] S.A. Kumar and S.M. Chen, *Sens. Actuators B* **123**, 964 (2007).
- [15] A. Azem, F. Man, and S. Omanovic, *J. Mol. Catal. A: Chem.* **219**, 283 (2004).
- [16] J.M. Jaksic, N.M. Ristic, N.V. Krstajic, and M.M. Jaksic, *Int. J. Hydrogen Energy* **23**, 1121 (1998).
- [17] H.Z. Wei and S. Omanovic, *Chem. Biodiv.* **5**, 1622 (2008).
- [18] W.F. Lin, M.S. Zei, Y.D. Kim, H. Over, and G. Ertl, *J. Phys. Chem. B* **104**, 6040 (2000).
- [19] M.A. El-Aziz and L.A. Kibler, *Electrochem. Commun.* **4**, 866 (2002).
- [20] M. Watanabe and S. Motoo, *J. Electroanal. Chem.* **60**, 267 (1975).
- [21] E. Herrero, K. Franaszczuk, and A. Wiecowski, *J. Electroanal. Chem.* **361**, 269 (1993).
- [22] A.J. Bard, *Electrochemical Methods, Fundamentals and Applications*, 2nd ed. (John Wiley & Sons, Inc, New York, 2000).
- [23] I.N. Levine, *Physical Chemistry*, 5th ed. (McGraw Hill, New York, 2002).
- [24] Eco Chemie B.V., General Purpose Electrochemical system, Version 4.9.5. Utrecht, The Netherlands.
- [25] M. Sharp, M. Petersson, and K. Edstrom, *J. Electroanal. Chem.* **95**, 123 (1979).
- [26] J. Moiroux and P.J. Elving, *J. Electroanal. Chem.* **102**, 93 (1979).